Electronegativity at the Shock Front

(article starts on next page)

Research Article

pep.wiley-vch.de

Electronegativity at the Shock Front

Martin Rahm*[a]

Dedicated to Karl O. Christe on the occasion of his 86th birthday.

Abstract: In this work, a scale for pressure-adapted atomic electronegativity is used to make general predictions of bond polarity in **H**-, **C**-, **N**- and **O**-based compounds experiencing shock conditions. The qualitative picture that emerges is one of increasing polarity of several bonds common in energetic materials. The general predictions made are compared to, and found to support, claims of ionic decomposition routes in compressed nitromethane and nitrate esters at high pressure. Changing electronegativity is also suggested as a factor driving the ionic disproportionation of various molecular phases with compression. Calculations using the eXtreme-Pressure Polarizable Continuum Model (XP-PCM) predict increasing energy differences between ground and excited states in non-bonded **H**, **C**, **N**, and **O** atoms as a function of pressure. This data enables for a discussion on the reliability of electronegativity-based rationales at more extreme thermodynamic conditions.

Keywords: Bond Polarity · Energetic Materials · Chemical Bonding · High Pressure

1 Introduction

This perspective article presents general predictions of bond polarity in molecules that experience shock compression. In conventional chemistry (at ambient conditions), realistic bond polarities can often be inferred from textbook tabulations of electronegativity. For example, chemists know to expect **O** to hold a negative charge when bonded to **C** because the former is more electronegative. A caveat often omitted is that at conditions of high-pressure atomic properties such as electronegativity, radii and even electron configuration can be different, and sometimes drastically so [1–3]. These changes can wreak havoc with our ability to rationalize or predict what may occur at different thermodynamic conditions. The purpose of this work is to highlight the availability and utility of an *existing* scale of atomic electronegativity adapted to high pressure [1–3].

Several different definitions of electronegativity have been proposed over the years (e.g., [4–9]). The resulting atomic scales typically show comparable trends across the periodic table and can often be interchangeably used to predict chemistry. However, few definitions are straightforwardly applicable to the study of compressed atoms. Our favored definition of electronegativity is the average binding energy of valence electrons [9]. This definition is similar, but not equal, to that of Allen [8], and allows (within certain approximations) for an extension to high pressure [1].

The arguments made herein assumes a simple premise: electronegativity is predictive of bond polarity. To make predictions following this premise, we rely on quantum mechanical calculations that describe isotropic compression of atoms by a non-reactive chemical environment resembling neon [1–3]. In other words, we rely on atomic properties that are provided *in the absence of chemical bonding*. This approach is analogous to how rationalization of chemical bonding under ambient conditions is often helped by comparison to atomic reference states.

We focus on four atom types: **H**, **C**, **N** and **O**. Extensive computational searches over stoichiometries of these atoms have predicted a plethora of phases forming under the immense pressures (100 s of GPa, 1 GPa ≈ 10,000 atm) of the interior of planets [10,11]. These same atoms are components of many energetic materials, which, when they detonate become subject to similar (albeit non-static) high-pressure conditions. Detonation pressures of conventional and state-of-the-art explosives range from ~20 GPa up to ~42 GPa (Figure 1) [12,13]. Even higher pressures, exceeding 100 GPa, have been predicted for as-of-yet hypothetical polynitrogen compounds [14].

The chemical dynamics of energetic materials experiencing conditions of shock are complex (see *e.g.*, [15–17]). It is well established that explosive-driven shock waves can alter reaction mechanisms [18,19], and it has been suggested that some ionic reactions are accelerated by compression. For example, at low-pressure nitrate esters decompose via homolysis of RO-NO₂ bonds, but at high static and shock pressures the bond cleavage becomes ionic and results in the formation of nitrate and carbocations [18,19]. The alteration of chemistry brought by compression is largely driven by changes to the underlying electronic structure and energy density of atoms and materials [20,21]. Shock-induced electrical activity has been reported

[a] *M. Rahm*
   Department of Chemistry and Chemical Engineering
   Chalmers University of Technology
   Kemigården 4, SE-412 96, Gothenburg, Sweden
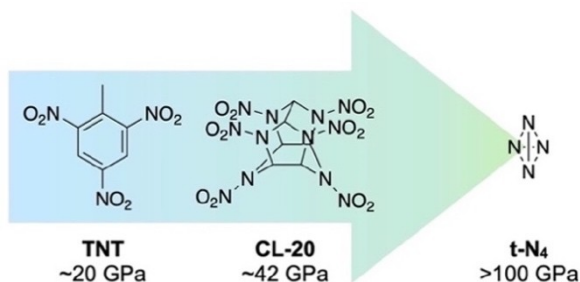   **e-mail: martin.rahm@chalmers.se*

Figure 1. Detonation of energetic materials is one way to explore the effect of high pressure on chemistry. Shown are trinitrotoluene (TNT), Hexanitrohexaazaisowurtzitane (CL-20) and tetrahedral nitrogen (t-N$_4$).

in energetic polymeric solids [22]. Local metallization of energetic compounds has been proposed to explain the often supersonic (> 8 km s^{-1}) and optically opaque reaction fronts [23].

Arguments based on electronegativity can fail, and sometimes do already at ambient conditions [24,25]. In what follows, we look to a scale of pressure-adapted electronegativity to improve our intuition of bond polarity in the extreme conditions of shock fronts. We also begin to address the reliability of predictions derived from electronegativity to the effects of temperature.

2 Methodology

The data underlying this work has been generated using the eXtreme-Pressure Polarizable Continuum Model (XP-PCM), an extension to high pressure of a method well-known in chemistry for treating solvent effects [26,27]. In the XP-PCM approach, the chemical environment surrounding an atom is modelled by a polarizable continuous medium defined in terms of a dielectric permittivity and a homogeneous electronic charge density. The atom to be compressed is placed in a cavity defined by a radius r_c. The total energy, $E(r_c)$, of the compressed system described by XP-PCM is expressed as

$$E(r_c) = < \Psi | \widehat{H}^o + \frac{1}{2} \widehat{V}_e + \widehat{V}_r | \Psi >, \qquad (1)$$

where Ψ is the wavefunction of the compressed atom, H^o is the Hamiltonian of the isolated atom, and $\widehat{V}_e$ and $\widehat{V}_r$ are operators describing electrostatic and Pauli repulsion interactions with the surrounding environment, respectively. The Pauli repulsion operator dominates the interaction between the atom and its environment, and it takes the form of a penetrable repulsive step potential located at the boundary of the cavity:

$$\widehat{V}_r = \int \widehat{\rho}(\mathbf{r}) Z \Theta(\mathbf{r}) d\mathbf{r} \quad \Theta(\mathbf{r}) = \begin{cases} 0 & \mathbf{r} \in \mathbf{C} \\ 1 & \mathbf{r} \notin \mathbf{C} \end{cases}, \qquad (2)$$

where $\widehat{\rho}(\mathbf{r}) = \sum_i^N \delta(\mathbf{r} - \mathbf{r}_i)$ is the electron density operator, N is the number of electrons in the system, Z is the height of the barrier potential, and $\Theta(\mathbf{r})$ is a spherical Heaviside unit step function that equals 0 inside the cavity $\mathbf{C}$ and 1 outside. Because this work largely relies on analysis of already published data, this method description is not exhaustive. Model parameters and further details on the cavity-dependence of Z is, for example, detailed elsewhere [26–29]. The interested reader is encouraged to study cited work for details beyond what is provided herein.

The pressure corresponding to a given cavity radius (and atomic property) can be calculated as the derivative of the electronic energy with respect to the confining cavity volume V_c [30]

$$p = -\left(\frac{\partial E}{\partial V_c} \right). \qquad (3)$$

An advantage of XP-PCM is that it, in principle, allows for any quantum mechanical level of theory. Other methods with similar capabilities to XP-PCM have been developed recently [31,32]. However, established options for modelling compression of single atoms, such as the helium compression chamber or matrix method [33], require large system sizes and the use of periodic boundary conditions. The latter approaches practically limit the level of theory to generalized gradient approximation-type density functional theory (DFT) calculations. Using XP-PCM, it is possible to rely on full-potential and relativistic treatment of atoms and on hybrid DFT methods at relatively moderate cost.

In this work, we analyze atomic properties calculated using the Perdew-Burke-Ernzerhof hybrid-exchange correlation functional PBE0 [34]. A Douglas-Kroll-Hess second-order scalar relativistic Hamiltonian [35–39] was used together with the very large and uncontracted atomic natural orbital-relativistic correlation consistent (ANO-RCC) basis set [40]. All calculations were done using a modified version of Gaussian 09 [41]. XP-PCM used together with this level of theory has been thoroughly benchmarked [1], e.g., by comparison to experimental T $\rightarrow$ 0 K compression isotherms [42] of elemental solids and shockwave experiments [2]. The approach effectively reproduces the properties of non-bonded atoms compressed by an environment most closely resembling that of neon.

With a quantum mechanical model in hand, it is possible to evaluate a range of properties, such as changing electronic ground states, size and electronegativity of compressed atoms [1–3]. Atomic electronegativity is here approximated from averages of energies of Kohn-Sham orbitals, as detailed elsewhere [1]. The reliability of electronegativity arguments at higher temperatures is in

Propellants Explos. Pyrotech. **2022**, e202100306 (2 of 7)

© 2022 Wiley-VCH GmbH

this work discussed with the help of computed energy differences between highest occupied and lowest unoccupied atomic orbitals as a function of pressure.

3 Results and Discussion

Figure 2 shows how the electronegativities of **C**, **N**, and **O** atoms are predicted to change as a function of pressure relative to **H**. To better highlight changes between these atoms with increasing pressure, Figure 2 is referenced to standard conditions of pressure (*i.e.*, where $p \approx 0$) [9]. The data in Figure 2 can be used to make the following *general* predictions for realistic (< 50 GPa) shock conditions (relative to ambient conditions):

1. **C−N**, **C−O**, **N−O**, **N−H**, and **O−H** bonds should become *more* polar, with an increasing negative charge on **O** before **N**.
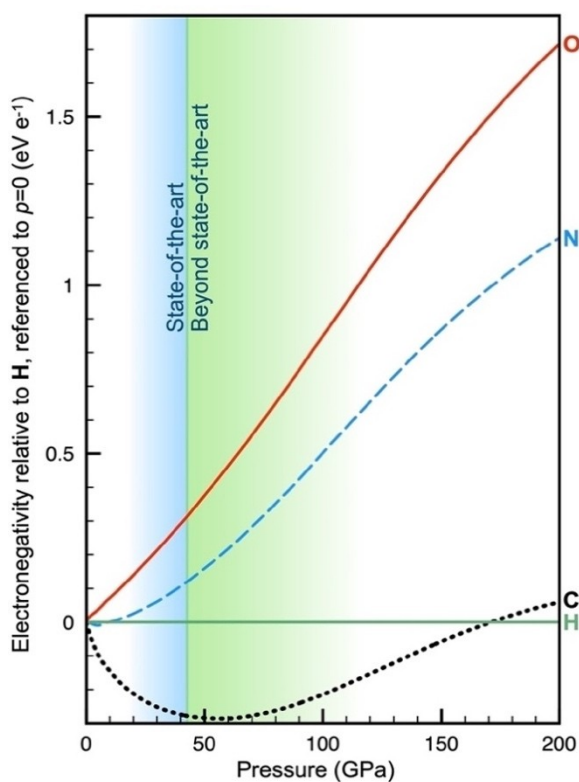2. Electron density in **C−H** bonds should shift more towards **H**.

Figure 2. Electronegativity of **C**, **O** and **N** relative to **H** as a function of pressure. The y-axis is referenced to conditions of zero pressure at which the electronegativity of these atoms are: **H**: 13.6, **C**: 13.9, **N**: 16.9, **O**: 18.6 eV e^{-1} (1 Pauling unit ≈ 6 eV e^{-1}) [9]. Ranges of detonation pressures in existing and hypothetical future materials are indicated in blue and green, respectively. State-of-the-art is here defined by the detonation pressure of CL-20. None of these atoms are predicted to undergo changes to their ground state electronic configurations in the relevant pressure range.

These predictions come with several caveats. As we will return to discuss, we should expect that electronic structures of molecules will occasionally override predictions based on simple descriptors like electronegativity. Furthermore, whereas we might expect a C−H bond to change its polarity from $C^{\delta-}-H^{\delta+} \rightarrow C^{\delta+}-H^{\delta-}$ with compression (*c.f.*, Figure 2), there is no unique method for quantifying atomic partial charges. Predictions of trends are more reliable than absolute calculations of polarity. Note also that the data shown in Figure 2 refer to atoms being non-reactively and hydrostatically compressed as $T \rightarrow 0$ K. How temperature may affect electronegativity is addressed in section 3.2 but is ignored in the following discussion.

To see how the general predictions of bond polarity hold up in real materials, we turn to literature. *Ab initio* methods have been used to study the effects of shocks on various energetic **H**-, **C**-, **N**- and **O**-containing compounds (*e.g.*, [43]). However, to the best of the author's knowledge, there is but one example that reports on trends in polarity of bonds in energetic materials in such conditions: high-pressure DFT molecular dynamics simulations of nitromethane, CH_3NO_2 [44]. These simulations have predicted an *increased* negative charge on **H** (i.e., in **C−H** bonds) with increasing pressure, and are thus seemingly in agreement with the evolution of electronegativity of these atoms with pressure.

The details of nitromethane decomposition are complex, debated, and outside the scope of this work to address in full. However, we note that Figure 2 also provides a possible explanation for some decomposition pathways supported both by *ab initio* DFT [44] and by **HCNO**-parametrized Density Functional Tight Binding (DFTB) simulations [45] of nitromethane: enhanced proton transfer with compression, forming $CH_3NO_2H^+$ and $CH_2NO_2^-$. These simulations both sampled conditions of tens of GPa and thousands of degrees.

The significant increase in the electronegativity of **O** with pressure predicts negative charge accumulation on this atom, which, in turn, should favor electrostatic interactions in materials, facilitating proton transfer. It, therefore, appears that knowledge of the pressure dependence of electronegativity and atom connectivity can suffice to qualitatively explain both reduction *and* oxidation of **H** in compressed nitromethane.

Simulation of realistic shock conditions is exceptionally computationally costly, and reactive force fields (*e.g.*, ReaxFF [15,17]) are commonly used instead of quantum mechanics. It should be noted that simulations of nitromethane using such methods disagree with the mentioned DFT and DFTB results. ReaxFF simulations predict nitromethane to decompose through unimolecular and neutral reaction mechanisms at similar conditions of compression [46]. It is possible that the latter methods struggle to capture the subtle electronic effects discussed herein, effects that have their origin in the changing nature of the atoms themselves with compression. For example, the forcefield

used to study nitromethane was parametrized against ground state molecules and is therefore unlikely to produce ionic species in simulations.

The XP-PCM model used to generate the data in Figure 2, accurately captures the full electronic response of compression on individual **H**, **C**, **N**, and **O** atoms, but leaves the mechanistic implications of such atomic properties on real materials up to speculation. In other words, *the predictive utility of atomic electronegativity computed for high pressure is at best as good as the conventional use of this central chemical concept.*

The predictions of changing bond polarity discussed in this work are agnostic with respect to material. As such, the general predictions exemplified using nitromethane apply equally to all materials containing the same bonds. For example, the same data may be used to rationalize the claimed preference for ionic decomposition of nitrate esters at high pressure [18, 19]. There are, additionally, several examples of pressure-induced formation of ionic phases from molecular solids that may find a partial explanation in the shifting electronegativity of atoms. For example, at high pressure water famously transforms into $[OH^-][H_3O^+]$ [47] and $[H^+]_2[O^{2-}]$ [48], and NH_3 into $[NH_4^+][NH_2^-]$ [49]. Other examples include the respective disproportionation of H_2S [50], NH_3H_2O, [51]' and N_2O [52]. The exact physical origins of such transformations are outside the scope of this work to determine. Here we postulate that the changing electronegativity of atoms may be one driving factor for such phenomena.

3.1 Other Atoms

Many other atom types can be present in energetic materials than the four discussed here. Complementary high-pressure data for 93 atoms is freely available in the online Atom-Under-Pressure Database [2, 53]. Using this database, we can explore what to expect from various kinds of metals commonly used as fuels in energetic compositions. Doing so makes apparent an exception-less rule: *all metal atoms become progressively less electronegative relative to **H** with increasing pressure.* This effect is larger for transition metal atoms (*e.g.*, **Ti** and **Fe**) and somewhat smaller for main group metal atoms such as **Al**.

An example of the opposite is **F**, a strong oxidant present in various energetic compounds (see *e.g.* [54–57]). The **F** atom follows a similar albeit stronger trend compared to **O** and **N** shown in Figure 2. The interested reader is encouraged to use the Atom-Under-Pressure Database [2, 53] to visualize this and any other atomic data.

3.2 The Effect of Temperature

Temperatures inside real detonations can soar well above ~ 5000 K. If one defines electronegativity as the average

binding energy of valence electrons [9], then this property is likely to be affected by electronic excitations to some degree. The lowest excited states of **H**, **C**, **N** and **O** lie 10.20, 1.26, 1.97, and 2.38 eV above their respective ground states [58]. Thermal excitation to such levels is unlikely even at 5000 K, where $kT \approx 0.43$ eV. However, photons generated by plasma in shock fronts are likely to enable such (mostly optical) transitions. Figure 3 shows XP-PCM calculations predicting *increasing* gaps between occupied and unoccupied levels in **H**, **C**, **N**, and **O** atoms with compression. Consequently, the effect of temperature on the properties of these *non-reactively compressed atomic reference systems* can be expected to *decrease* with pressure.

Energy gaps in real bonded materials are another matter entirely: in compressed condensed phase systems, levels formally belonging to different molecules or atoms interact. The enlarged dispersion of valence and conduction bands resulting from pressure conspire to lower optical band gaps, and will, eventually, lead to metallization. Figure 3 suggests that increases of energy gaps in atomic non-bonded reference states with pressure may partially counteract the gap-lowering effect associated with band dispersion in bonded systems. The degree to which such cancellation can occur will vary between materials. *Ab initio* molecular dynamics simulations of shocked nitromethane reportedly do not produce a significant population of excited states [59, 60]. The band gap of shocked HMX remains large up to 90 GPa, and metallization is only predicted past 120 GPa [61]. In other words, the bandgap of several energetic materials can stay relatively large in realistic shock front conditions despite both compression and heating. These exam-
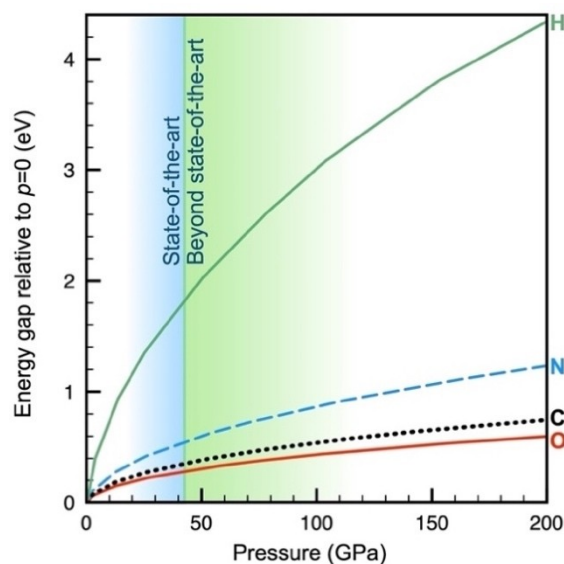
Figure 3. Increasing energy differences between ground state and excited state atoms as a function of pressure. Trends are estimated from changing energy gaps between lowest unoccupied and highest occupied atomic Kohn-Sham orbitals.

ples, focused on **H**, **C**, **N** and **O**, suggest that arguments based on pressure-resolved electronegativity can remain valid even in extreme conditions of temperature and pressure. Nevertheless, electronegativity arguments are expected to weaken when excited states of atoms come sufficiently down in energy to be significantly populated. Such tendencies are predicted to occur for the compression of several alkali, alkaline earth, transition metal, lanthanide, and actinide atoms, but not for atoms of the main group [1].

4 Conclusion

In this work, we analyze an established scale of pressure-resolved atomic electronegativity to build chemical intuition for what to expect of chemistry in shock fronts. The effect of high pressure on chemistry is often profound, and arguably more straightforward to explore in static conditions, *e.g.*, with the use of diamond anvil cells. However, by considering the dynamic processes of detonations and focusing on four atom types, **H**, **C**, **N**, and **O**, it is possible to make predictions of bond polarity and compare these against research on energetic materials. Established trends in polarities of chemical bonds and preferences for ionic decomposition routes in nitrate esters and nitromethane at high pressure are found to be qualitatively explainable from the evolution of electronegativity with pressure. **O** and **N** will grow progressively more electronegative relative to **C** and **H** as pressure builds. The studied atomic data also appear in agreement with preferences for ionic disproportionation in various high-pressure phases of small molecules. The XP-PCM method is used to estimate the energies of excited states of **H**, **C**, **N** and **O** as a function of pressure. These calculations support the utility of the simple yet central chemical concept of electronegativity even at high temperature. The qualitative and general trends proposed herein are suggested as a guide for what to expect when energetic materials are subjected to high pressures.

5 Symbols and Abbreviations

TNT   2,4,6-trinitrotoluene
HMX   1,3,5,7-Tetranitro-1,3,5,7-tetrazocane
CL-20 Hexanitrohexaazaisowurtzitane
t-N_4 tetrahedral nitrogen

Acknowledgements

Data Availability Statement

Most data that support the findings of this study are openly available in an online database found at: https://rahmlab.com/atoms-under-pressure/ Other data are available upon reasonable request to the author.

References

[1] M. Rahm, R. Cammi, N. W. Ashcroft, R. Hoffmann, Squeezing All Elements in the Periodic Table: Electron Configuration and Electronegativity of the Atoms under Compression, *J. Am. Chem. Soc.* **2019**, *141*, 10253–10271.

[2] M. Rahm, M. Ångqvist, J. M. Rahm, P. Erhart, R. Cammi, Non-bonded Radii of the Atoms Under Compression, *ChemPhysChem* **2020**, *21*, 2441–2453.

[3] M. Rahm, P. Erhart, R. Cammi, Relating atomic energy, radius and electronegativity through compression, *Chem. Sci.* **2021**, *12*, 2397–2403.

[4] L. Pauling, Nature of the chemical bond. IV. The energy of single bonds and the relative electronegativity of atoms., *J. Am. Chem. Soc.* **1932**, *54*, 3570–3582.

[5] R. S. Mulliken, New electroaffinity scale; together with data on valence states and on valence ionization potentials and electron affinities., *J. Chem. Phys.* **1934**, *2*, 782–793.

[6] A. L. Allred, E. G. Rochow, A scale of electronegativity based on electrostatic force., *J. Inorg. Nucl. Chem.* **1958**, *5*, 264–268.

[7] R. G. Parr, R. A. Donnelly, M. Levy, W. E. Palke, Electronegativity: The density functional viewpoint., *J. Chem. Phys.* **1978**, *68*, 3801–3807.

[8] L. C. Allen, Electronegativity is the average one-electron energy of the valence-shell electrons in ground-state free atoms., *J. Am. Chem. Soc.* **1989**, *111*, 9003–9014.

[9] M. Rahm, T. Zeng, R. Hoffmann, Electronegativity Seen as the Ground-State Average Valence Electron Binding Energy, *J. Am. Chem. Soc.* **2019**, *141*, 342–351.

[10] A. S. Naumova, S. V. Lepeshkin, P. V. Bushlanov, A. R. Oganov, Unusual Chemistry of the C—H—N—O System under Pressure and Implications for Giant Planets, *J. Phys. Chem. A* **2021**, *125*, 3936–3942.

[11] L. J. Conway, C. J. Pickard, A. Hermann, Rules of formation of H—C—N—O compounds at high pressure and the fates of planetary ices, *Proc Natl Acad Sci USA* **2021**, *118*, e2026360118.

[12] A. Baxter, F. I. Martin, K. O. Christe, R. Haiges, Formamidinium Nitroformate: An Insensitive RDX Alternative, *J. Am. Chem. Soc.* **2018**.

[13] K. O. Christe, D. A. Dixon, M. Vasiliu, R. Haiges, B. Hu, How Energetic are cyclo-Pentazolates?, *Propellants Explos. Pyrotech.* **2018**, *140*, 15089–15098.

[14] H. Östmark, S. Walin, P. Goede, High energy density materials (HEDM): overview, theory and synthetic efforts at FOI., *Cent. Eur. J. Energ. Mater.* **2007**, *4*, 83–108.

[15] A. Strachan, A. C. T. van Duin, D. Chakraborty, S. Dasgupta, W. A. Goddard, Shock Waves in High-Energy Materials: The Initial Chemical Events in Nitramine RDX, *Phys. Rev. Lett.* **2003**, *91*, 098301.

[16] M. R. Manaa, L. E. Fried, The reactivity of energetic materials under high pressure and temperature., *Adv. Quantum Chem.* **2014**, *69*, 221–252.

[17] F. Wang, L. Chen, D. Geng, J. Lu, J. Wu, Molecular Dynamics Simulations of an Initial Chemical Reaction Mechanism of

Shocked CL-20 Crystals Containing Nanovoids, *J. Phys. Chem. C* **2019**, *123*, 23845–23852.

[18] D. L. Naud, K. R. Brower, Pressure effects on the thermal decomposition of nitramines, nitrosamines, and nitrate esters., *J. Org. Chem.* **1992**, *57*, 3303–3308.

[19] L. L. Davis, K. R. Brower, Reactions of Organic Compounds in Explosive-Driven Shock Waves., *J. Phys. Chem.* **1996**, *100*, 18775–18783.

[20] W. Grochala, R. Hoffmann, J. Feng, N. W. Ashcroft, The chemical imagination at work in very tight places., *Angew. Chem. Int. Ed.* **2007**, *46*, 3620–3642; *Angew. Chem.* **2007**, *119*, 3694–3717.

[21] M. Miao, Y. Sun, E. Zurek, H. Lin, Chemistry under high pressure, *Nat. Chem. Rev.* **2020**, *4*, 508–527.

[22] R. A. Graham, Shock-induced electrical activity in polymeric solids. A mechanically induced bond scission model., *J. Phys. Chem.* **1979**, *83*, 3048–3056.

[23] J. J. Gilman, Chemical reactions at detonation fronts in solids., *Philos. Mag. B* **1995**, *71*, 1057–1068.

[24] G. Frenking, C. Loschen, A. Krapp, S. Fau, S. H. Strauss, Electronic structure of CO – An exercise in modern chemical bonding theory, *J. Comput. Chem.* **2007**, *28*, 117–126.

[25] S. Racioppi, M. Rahm, In-Situ Electronegativity and the Bridging of Chemical Bonding Concepts, *Chem. Eur. J.* **2021**, *27*, 18156–18167.

[26] R. Cammi, A new extension of the polarizable continuum model: Toward a quantum chemical description of chemical reactions at extreme high pressure., *J. Comput. Chem.* **2015**, *36*, 2246–2259.

[27] R. Cammi, Quantum Chemistry at the High Pressures: The eXtreme Pressure Polarizable Continuum Model (XP-PCM), in Frontiers of Quantum Chemistry, **2018**, 273–287.

[28] J. Tomasi, B. Mennucci, R. Cammi, Quantum Mechanical Continuum Solvation Models., *Chem. Rev.* **2005**, *105*, 2999–3093.

[29] C. Amovilli, B. Mennucci, Self-Consistent Field Calculation of Pauli Repulsion and Dispersion Contributions to the Solvation Free Energy in the Polarizable Continuum Model., *J. Phys. Chem. B* **1997**, *101*, 1051–1057.

[30] R. Cammi, B. Chen, M. Rahm, Analytical calculation of pressure for confined atomic and molecular systems using the eXtreme-Pressure Polarizable Continuum Model, *J. Comb. Chem.* **2018**, *39*, 2243–2250.

[31] M. Scheurer, A. Dreuw, E. Epifanovsky, M. Head-Gordon, T. Stauch, Modeling Molecules under Pressure with Gaussian Potentials, *J. Chem. Theory Comput.* **2021**, *17*, 583–597.

[32] T. Stauch, A mechanochemical model for the simulation of molecules and molecular crystals under hydrostatic pressure, *J. Chem. Phys.* **2020**, *153*, 134503.

[33] M.-S. Miao, R. Hoffmann, High Pressure Electrides: A Predictive Chemical and Physical Theory., *Acc. Chem. Res.* **2014**, *47*, 1311–1317.

[34] C. Adamo, V. Barone, Toward reliable density functional methods without adjustable parameters: the PBE0 model., *J. Chem. Phys.* **1999**, *110*, 6158–6170.

[35] M. Douglas, N. M. Kroll, Quantum electrodynamical corrections to the fine structure of helium., *Ann. Phys.* **1974**, *82*, 89–155.

[36] B. A. Hess, Applicability of the no-pair equation with free-particle projection operators to atomic and molecular structure calculations., *Phys. Rev. A* **1985**, *32*, 756–763.

[37] B. A. Hess, Relativistic electronic-structure calculations employing a two-component no-pair formalism with external-field projection operators., *Phys. Rev. A* **1986**, *33*, 3742–3748.

[38] M. Barysz, A. J. Sadlej, Two-component methods of relativistic quantum chemistry: from the Douglas-Kroll approximation to the exact two-component formalism., *J. Mol. Struct.* **2001**, *573*, 181–200.

[39] W. A. de Jong, R. J. Harrison, D. A. Dixon, Parallel Douglas-Kroll energy and gradients in NWChem: Estimating scalar relativistic effects using Douglas-Kroll contracted basis sets., *J. Chem. Phys.* **2001**, *114*, 48–53.

[40] P. O. Widmark, P. Malmqvist, B. O. Roos, Density matrix averaged atomic natural orbital (ANO) basis sets for correlated molecular wave functions. I. First row atoms., *Theor. Chim. Acta* **1990**, *77*, 291–306.

[41] M. J. Frisch, G. W. Trucks, H. B. Schlegel, G. E. Scuseria, M. A. Robb, J. R. Cheeseman, G. Scalmani, V. Barone, B. Mennucci, G. A. Petersson, H. Nakatsuji, M. Caricato, X. Li, H. P. Hratchian, A. F. Izmaylov, J. Bloino, G. Zheng, J. L. Sonnenberg, M. Hada, M. Ehara, K. Toyota, R. Fukuda, J. Hasegawa, M. Ishida, T. Nakajima, Y. Honda, O. Kitao, H. Nakai, T. Vreven, J. J. A. Montgomery, J. E. Peralta, F. Ogliaro, M. Bearpark, J. J. Heyd, E. Brothers, K. N. Kudin, V. N. K. Staroverov, R. J. Normand, K. Raghavachari, A. Rendell, J. C. Burant, S. S. Iyengar, J. Tomasi, M. Cossi, N. Rega, N. J. Millam, M. Klene, J. E. Knox, J. B. Cross, V. Bakken, C. Adamo, J. Jaramillo, R. Gomperts, R. E. Stratmann, O. Yazyev, A. J. Austin, R. Cammi, C. Pomelli, J. W. Ochterski, R. L. Martin, K. Morokuma, V. G. Zakrzewski, G. A. Voth, P. Salvador, J. J. Dannenberg, S. Dapprich, A. D. Daniels, Ö. Farkas, J. B. Foresman, J. V. Ortiz, J. Cioslowski, D. J. Fox, *Gaussian 09, Revision A.02*, Gaussian, Inc., Wallingford CT, **2009**.

[42] D. A. Young, H. Cynn, P. Söderlind, A. Landa, Zero-Kelvin Compression Isotherms of the Elements $1 \leq Z \leq 92$ to 100 GPa., *J. Phys. Chem. Ref. Data* **2016**, *45*, 043101/1–043101/36.

[43] C. H. Pham, R. K. Lindsey, L. E. Fried, N. Goldman, Calculation of the detonation state of HN_3 with quantum accuracy., *J. Chem. Phys.* **2020**, *153*, 224102.

[44] M. R. Manaa, E. J. Reed, L. E. Fried, G. Galli, F. Gygi, Early chemistry in hot and dense nitromethane: molecular dynamics simulations, *J. Chem. Phys.* **2004**, *120*, 10146–10153.

[45] R. Perriot, M. J. Cawkwell, E. Martinez, S. D. McGrane, Reaction Rates in Nitromethane under High Pressure from Density Functional Tight Binding Molecular Dynamics Simulations., *J. Phys. Chem. A* **2020**, *124*, 3314–3328.

[46] N. Rom, S. V. Zybin, A. C. T. van Duin, W. A. Goddard, III, Y. Zeiri, G. Katz, R. Kosloff, Density-Dependent Liquid Nitromethane Decomposition: Molecular Dynamics Simulations Based on ReaxFF., *J. Phys. Chem. A* **2011**, *115*, 10181–10202.

[47] Y. Wang, H. Liu, J. Lv, L. Zhu, H. Wang, Y. Ma, High pressure partially ionic phase of water ice, *Nat. Commun.* **2011**, *2*, 563.

[48] M. Millot, F. Coppari, J. R. Rygg, A. Correa Barrios, S. Hamel, D. C. Swift, J. H. Eggert, Nanosecond X-ray diffraction of shock-compressed superionic water ice, *Nature* **2019**, *569*, 251–255.

[49] C. J. Pickard, R. J. Needs, Highly compressed ammonia forms an ionic crystal, *Nat. Mater.* **2008**, *7*, 775–779.

[50] R. Rousseau, M. Boero, M. Bernasconi, M. Parrinello, K. Terakura, Ab initio Simulation of Phase Transitions and Dissociation of H_2S at High Pressure, *Phys. Rev. Lett.* **2000**, *85*, 1254–1257.

[51] A. D. Fortes, J. P. Brodholt, I. G. Wood, L. Vočadlo, H. D. B. Jenkins, Ab initio simulation of ammonia monohydrate ($NH_3 \cdot H_2O$) and ammonium hydroxide (NH_4OH), *J. Chem. Phys.* **2001**, *115*, 7006–7014.

[52] M. Somayazulu, A. Madduri, A. F. Goncharov, O. Tschauner, P. F. McMillan, H.-k. Mao, R. J. Hemley, Novel Broken Symmetry Phase from H_2S at High Pressures and High Temperatures, *Phys. Rev. Lett.* **2001**, *87*, 135504.

[53] The Atoms Under Pressure (AUP) database is available at: https://www.rahmlab.com/atoms-under-pressure/

[54] K. O. Christe, W. W. Wilson, C. J. Schack, R. D. Wilson, Tetra-fluoroammonium salts., *Inorg. Synth.* **1986**, *24*, 39–48.

[55] G. A. Olah, N. Hartz, G. Rasul, Q. Wang, G. K. S. Prakash, J. Casanova, K. O. Christe, Electrophilic Fluorination of Methane with "F$^+$" Equivalent N$_2$F$^+$ and NF$_4^+$ Salts, *J. Am. Chem. Soc.* **1994**, *116*, 5671–5673.

[56] K. O. Christe, D. A. Dixon, D. J. Grant, R. Haiges, F. S. Tham, A. Vij, V. Vij, T.-H. Wang, W. W. Wilson, Dinitrogen Difluoride Chemistry. Improved Syntheses of cis- and *trans*-N$_2$F$_2$, Synthesis and Characterization of N$_2$F$^+$Sn$_2$F$_9^-$, Ordered Crystal Structure of N$_2$F$^+$Sb$_2$F$_{11}^-$, High-Level Electronic Structure Calculations of *cis*-N$_2$F$_2$, *trans*-N$_2$F$_2$, F$_2$N=N, and N$_2$F$^+$, and Mechanism of the trans–cis Isomerization of N$_2$F$_2$, *Inorg. Chem.* **2010**, *49*, 6823–6833.

[57] K. O. Christe, W. W. Wilson, G. Belanger-Chabot, R. Haiges, J. A. Boatz, M. Rahm, G. K. S. Prakash, T. Saal, M. Hopfinger, Synthesis and Characterization of Fluorodinitroamine, FN(NO$_2$)$_2$., *Angew. Chem. Int. Ed.* **2015**, *54*, 1316–1320; *Angew. Chem.* **2015**, *127*, 1332–1336.

[58] Unless otherwise noted, all experimental data were obtained from the NIST Standard Reference Database Number 69, which can be accessed electronically through the NIST Chemistry Web Book (http://webbook.nist.gov/chemistry/); references are given therein.

[59] E. J. Reed, J. D. Joannopoulos, L. E. Fried, Electronic excitations in shocked nitromethane., *Phys. Rev. B: Condens. Matter Mater. Phys.* **2000**, *62*, 16500–16509.

[60] E. J. Reed, M. Riad Manaa, L. E. Fried, K. R. Glaesemann, J. D. Joannopoulos, A transient semimetallic layer in detonating nitromethane., *Nat. Phys.* **2008**, *4*, 72–76.

[61] N.-N. Ge, Y.-K. Wei, F. Zhao, X.-R. Chen, G.-F. Ji, Pressure-induced metallization of condensed phase β-HMX under shock loadings via molecular dynamics simulations in conjunction with multi-scale shock technique., *J. Mol. Model.* **2014**, *20*, 1–9.
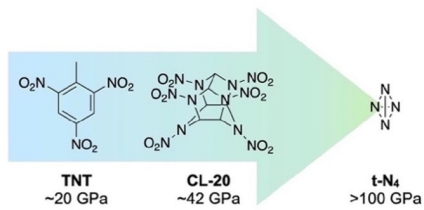
M. Rahm*

1 – 8

Electronegativity at the Shock Front